TUDCA protects against tunicamycin-induced apoptosis of dorsal root ganglion neurons by suppressing activation of ER stress

FANGYI CHEN[1], ZHE GE[1], NAN LI[2], ZUOCHONG YU[1], RONGBO WU[1], YAN ZHAO[3], XIANWEI HE[1] and GUOPING CAI[1]

Departments of [1]Orthopedics, [2]Stomatology and [3]Clinical Laboratory, Jinshan Hospital, Fudan University, Shanghai 201508, P.R. China

Received February 4, 2022; Accepted May 5, 2022

DOI: 10.3892/etm.2022.11436

Abstract. The existence of endoplasmic reticulum (ER) stress in neurodegenerative diseases has been well established. Tauroursodeoxycholic acid (TUDCA) is a bile acid taurine conjugate derived from ursodeoxycholic acid, which has been reported to exert cytoprotective effects on several types of cells by inhibiting ER stress. The present study explored the effects of TUDCA on primary cultured rat dorsal root ganglion (DRG) neurons. Cell viability and apoptosis of DRG neurons treated with TUDCA and tunicamycin were detected by CellTiter-Blue assay and TUNEL staining, respectively. The protein levels and phosphorylation of apoptosis and ERS-related signaling pathway molecules were detected by western blot, and the mRNA levels of related genes were assessed by reverse transcription-quantitative PCR. Notably, TUDCA had no significant cytotoxic effect on DRG neurons at concentrations ≤250 μM. In addition, the apoptosis induced by tunicamycin exposure was markedly suppressed by TUDCA, as indicated by the percentage of TUNEL-positive cells, the activities of caspases and the changes in expression levels of critical apoptosis factors. Furthermore, the cytotoxicity of tunicamycin in DRG neurons was accompanied by an increase in malondialdehyde (MDA) content, reactive oxygen species (ROS) and lactate dehydrogenase (LDH) production, and a decrease in glutathione (GSH) levels. The changes in oxidative stress-related factors (ROS, LDH, MDA and GSH) were reversed by TUDCA. Furthermore, as determined by western blotting, the increase in C/EBP homologous protein, glucose-regulated protein 78 and cleaved caspase-12 expression following tunicamycin treatment suggested the activation of ER stress. Downregulation of ER stress components and unfolded protein response sensors by TUDCA confirmed the implication of ER stress in the effects of TUDCA on DRG neurons. In conclusion, the present study indicated that TUDCA may protect against tunicamycin-induced DRG apoptosis by suppressing the activation of ER stress. The protective effect and the therapeutic value of TUDCA in nervous system injury require further study in animal models.

Correspondence to: Dr Xianwei He or Dr Guoping Cai, Department of Orthopedics, Jinshan Hospital, Fudan University, 1508 Longhang Road, Shanghai 201508, P.R. China
E-mail: xianwhe@126.com
E-mail: guopcai@126.com

Key words: tauroursodeoxycholic acid, tunicamycin, dorsal root ganglia, endoplasmic reticulum stress, apoptosis

Introduction

Tauroursodeoxycholic acid (TUDCA) is a bile acid taurine conjugate derived from ursodeoxycholic acid, which is naturally occurring in the body. TUDCA has been approved by the U.S. Food and Drug Administration to treat primary biliary cholangitis, and shows good safety and effectiveness in clinical practice (1). In addition to its choleretic activity and protective role in hepatocytes, TUDCA has been shown to inhibit endoplasmic reticulum (ER) stress, regulate mitochondrial dysfunction, suppress cellular apoptosis and decrease inflammation in various disease models (2-5). Despite evidence demonstrating the beneficial effects of TUDCA in pre-clinical studies, the underlying mechanisms are not fully understood.

ER stress has been demonstrated to contribute to the development and progression of a number of diseases, including nerve injury (6,7), degenerative diseases of the nervous system (8), diabetes (9), cardiovascular (10) and liver diseases (11,12), and cancer (13). Therefore, ER stress has been recognized as an emerging target for therapy. Evidence from preclinical studies has suggested that targeting ER stress components or different unfolded protein response (UPR) signaling branches through gene therapy or pharmacological approaches can delay neurodegeneration (14-16). Apoptosis of dorsal root ganglion (DRG) neurons has been reported in animal models of peripheral nerve injury (17). Studies of animal models with sciatic nerve transection have shown increased levels of caspase-3, caspase-8, caspase-12 and caspase-7 in the DRG, and phosphorylated (p)-protein kinase R-like ER kinase (PERK) has been observed to mainly colocalize with isolectin B4-positive neurons in the DRG (18). In support of this, a previous study demonstrated that the ER stress-mediated apoptotic pathways were activated in the injured DRG and contributed to the development of pain hypersensitivity after nerve injury (6). Therefore, pathogenic

ER stress of the DRG has been recognized as an emerging target for peripheral nerve injury therapy.

The present study investigated the effects of TUDCA on ER stress-associated apoptosis induced by tunicamycin in primary cultured rat DRG neurons. Cell viability, caspase activity, oxidative stress-related factors and activation of ER stress pathways in DRG cells were studied, and the anti-apoptotic effect and potential mechanism of TUDCA in DRG neurons was reported.

Materials and methods

Chemicals and reagents. Neurobasal medium, B-27, nerve growth factor (NGF), penicillin-streptomycin and trypsin were obtained from Thermo Fisher Scientific, Inc. Poly-D-lysine, tunicamycin, laminin, collagenase and 5-fluoro-2'-deoxyuridine (FUDR) were purchased from MilliporeSigma. TUDCA and thapsigargin were obtained from Selleck Chemicals and dissolved in DMSO. Antibodies used in immunofluorescence staining and western blotting are listed in Table SI.

DRG neurons culture and treatment. Pregnant Sprague-Dawley rats (10-15 weeks old) were provided by Beijing Vitalstar Biotechnology Co., Ltd. A total of 10 pregnant rats and 107 embryonic rats were used for DRG collection in this study. Rats were maintained in plastic cages under controlled conditions, with an ambient temperature of 23˚C and 50% relative humidity, with free access to food and water. Rats were placed in a room with a standard 12-h light/dark cycle. Pregnant rats were euthanized by CO_2 inhalation in the home cage with a flow rate of 30% displacement of cage volume/min. DRG neurons were isolated and cultured as previously described (19,20). In brief, the DRG was harvested from Sprague-Dawley rats at embryonic day 15 or 16 and digested with 0.25% trypsin and 0.3% collagenase type I at 37˚C for 25 min. DRG neurons were then dissociated by repetitive pipetting and cells were centrifuged at 200 x g at room temperature for 5 min. Cells were resuspended in neurobasal medium supplemented with 2% B-27, 10 ng/ml NGF and penicillin-streptomycin (both 100 μg/ml), and seeded into 96-well plates precoated with poly-D-lysine and laminin. DRG neurons were cultured at 37˚C with 5% CO_2 and medium was replaced every day, cycled on media with or without 20 μM FUDR for a total of 10 days to deplete non-neuronal cells. DRG neurons were identified with antibodies against β-tubulin and neurofilament 200 (NF200).

Cell viability detection. Cell viability of DRG neurons was evaluated using CellTiter-Blue Cell Viability assay (Promega Corporation). DRG neurons were cultured in 96-well plates ($5x10^4$ cells/well) and pretreated with different doses of TUDCA (50, 100, 250, 500 and 1,000 μM) at 37˚C for 24 h. Medium was then replaced with fresh medium containing tunicamycin (0.75 μg/ml) or thapsigargin (1 μM) and incubated at 37˚C for another 24 h.

Following treatment, CellTiter-Blue reagent was added directly to each well (20 μl/well) and the plate was agitated for 10 sec and incubated at 37˚C for 1 h before measuring fluorescence ($560_{Ex}/590_{Em}$) using a multimode plate reader (Thermo Fisher Scientific Inc.). Each assay was repeated at least three times. Cell viability was shown as a percentage of the control group.

Immunofluorescent staining. DRG neurons were fixed with 4% paraformaldehyde for 30 min at room temperature before immunofluorescent staining. For β-tubulin, glial fibrillary acidic protein (GFAP), ionized calcium binding adaptor molecule 1 (Iba1) and NF200 staining, cells were blocked with 3% BSA (Beyotime Institute of Biotechnology) containing 0.1% Triton X-100 and 10% goat serum (Beyotime Institute of Biotechnology) for 1 h at room temperature to avoid non-specific staining. The cells were then incubated with primary antibodies against β-tubulin (1:200), GFAP (1:200), Iba1 (1:800) or NF200 (1:200) overnight at 4˚C, and incubated with Alexa Fluor 488- or Alexa Fluor 633-conjugated secondary antibodies for 2 h at room temperature and stained with DAPI for 10 min at room temperature. For the TUNEL assay, DRG neurons were washed with PBS and blocked with 3% H_2O_2 in methanol for 10 min at room temperature and permeabilized with 0.5% Triton X-100 for 5 min at room temperature. Neurons were then incubated in the dark with 50 μl TUNEL reaction mixture (Beyotime Institute of Biotechnology) for 1 h at 37˚C. TUNEL-positive cells were observed with a Leica confocal microscope (Leica Microsystems GmbH). A minimum of 10 random fields of view was observed by microscopy.

Caspase activity assay. Caspase activity of DRG neurons was assessed using Caspase-Glo System (Promega Corporation) according to the manufacturer's protocol. DRG neurons were plated in white-walled 96-well plates and treated with or without TUDCA and/or tunicamycin. Caspase-Glo Reagent was then added to the cells (100 μl/well) and mixed well. Luminescence of each sample was measured using a luminometer (Thermo Fischer Scientific, Inc.) after incubation at room temperature for 1 h. Results were calculated as signal-to-noise ratios and the relative activities were shown as ratios of the control group.

Quantification of lactate dehydrogenase (LDH). LDH release in the culture supernatant of DRG neurons was determined using the LDH Cytotoxicity Detection Kit (Takara Bio, Inc.). The cell culture supernatant was collected and transferred to a clear, flat-bottom microtiter plate after treatment, 100 μl reaction mixture was added to each well and the plate was incubated in the dark for 25 min at room temperature. The reaction was stopped by adding 1N HCl to each well. LDH release was measured at 490 nm using a multimode plate reader (Thermo Fisher Scientific, Inc.). Each assay was repeated at least three times. Relative LDH level was shown as a percentage of the untreated control.

ROS detection. For ROS detection, cell culture medium of DRG neurons was removed and 50 μl 2',7'-dichlorofluorescein diacetate (DCFH-DA) (10 μM; Beyotime Institute of Biotechnology) was added to each well (20 μl/well). Cells (10,000/well) were incubated at 37˚C for 20 min and were then washed thoroughly to remove the DCFH-DA that did not enter the cells. Fluorescence ($490_{Ex}/525_{Em}$) was detected using a multimode plate reader (Thermo Fisher Scientific, Inc.).

Malondialdehyde (MDA) detection assay. Different concentrations of standards were used to make a standard curve. Subsequently, 0.2 ml MDA detection working solution (Beyotime Institute of Biotechnology) was added to each sample. After mixing, the samples were boiled for 15 min and cooled to room temperature in a water bath, then centrifuged at 1,000 x g for 10 min at room temperature. The supernatant was moved to a new 96-well plate and absorbance was measured at 532 nm using a microplate reader (Thermo Fisher Scientific, Inc.). The concentration of MDA was calculated according to the standard curve and the relative MDA levels were compared with the untreated group.

Glutathione (GSH) detection assay. GSH production was determined using a GSH detection assay kit (Beyotime Institute of Biotechnology). After treatment, DRG neurons (10,000/well) were washed once with PBS and the supernatant was removed. Protein removal reagent S solution (30 μl/well) was added to the cells and vortexed. Subsequently, liquid nitrogen and a 37˚C water bath were used to freeze and thaw the samples twice. Samples were placed at 4˚C for 5 min and centrifuged at 10,000 x g for 10 min. The supernatant was then used for the determination of GSH. Briefly, GSH detection working solution (150 μl/well) was added to standards and samples, mixed well and incubated at room temperature for 5 min. Subsequently, 50 μl NADPH solution (0.5 mg/ml) was added to wells and mixed, and absorbance at 412 nm was immediately determined using a multimode plate reader. Different concentrations of standards were used to make a standard curve. GSH concentration was calculated by comparing the sample to the standard curve.

Reverse transcription-quantitative PCR (RT-qPCR). Total RNA was extracted from DRG neurons using TRIzol® (Invitrogen; Thermo Fisher Scientific, Inc.) and cDNA was generated using PrimeScript RT Reagent Kit (cat. no. RR037B; Takara Bio, Inc.) according to the manufacturer's protocol. Changes in mRNA expression were measured using the SYBR Green Realtime PCR Master Mix kit (cat. no. QPK-201; Toyobo Life Science). The amplification started with an initial denaturation step at 95˚C for 60 sec, followed by 40 cycles of denaturation at 95˚C for 15 sec, annealing at 60˚C for 15 sec and extension at 72˚C for 45 sec. Relative expression levels of target genes were calculated using the $2^{-\Delta\Delta Cq}$ method and normalized to β-actin of respective samples (21). The primers used in this study are listed in Table SII.

Western blot analysis. DRG neurons were harvested and lysed using RIPA lysis buffer (Beyotime Institute of Biotechnology) supplemented with a protease and phosphatase inhibitor cocktail (CoWin Biosciences). Bicinchoninic acid assay kit (Pierce; Thermo Fisher Scientific, Inc.) was used to quantify protein concentrations, and equal amounts of protein (30 μg) were separated by SDS-PAGE and transferred onto PVDF membranes (Millipore). Subsequently, the membrane was blocked with 5% non-fat milk for 2 h at room temperature and then incubated with primary antibodies overnight at 4˚C. After incubation with HRP-conjugated antibodies for 2 h at room temperature, protein expression was visualized by ECL Western Blotting Substrate (Pierce; Thermo Fisher Scientific, Inc.) and semi-quantified using a Bio-Rad imaging system (Image Lab software 4.0; Bio-Rad Laboratories, Inc.).

Statistical analysis. All data are presented as the mean ± SEM. Statistical analysis was performed using one-way ANOVA and Tukey test using GraphPad Prism 7.0 (GraphPad Software, Inc.). $P<0.05$ was considered to indicate a statistically significant difference. Each experiment was repeated at least three times.

Results

Effect of TUDCA on the viability of DRG neurons. Double immunofluorescence staining of DRG neurons derived from rat fetuses was performed to confirm the purity of the cells. DRG neurons were positive for β-tubulin and NF200 (Fig. 1A). Iba1-labeled resident macrophages and GFAP-positive glial cells were not observed (Fig. 1A). The purity of DRG neurons was >90%.

To explore the effect of TUDCA on DRG neurons, cultures were incubated with medium containing various concentrations (0, 50, 100, 250, 500 and 1,000 μM) of TUDCA for 24 h and the cell viability was detected by CellTiter-Blue assay. TUDCA had no significant cytotoxic effect on DRG neurons at low concentrations (50, 100 and 250 μM). There was a marked reduction in cell viability when the concentration of TUDCA was ≥500 μM. Cell viability of DRG neurons decreased by 20% after exposure to 1,000 μM TUDCA compared with that of untreated cells (Fig. 1B). Subsequently, the cytoprotective effect of TUDCA against tunicamycin-induced cytotoxicity was evaluated. A 24-h incubation with 0.75 μg/ml tunicamycin significantly decreased the viability of DRG neurons; this was reversed by TUDCA at the concentrations of 250 and 500 μM (Fig. 1C). Since TUDCA had no effect on cell viability of DRG neurons at 250 μM, this concentration was used in the subsequent experiments.

Effect of TUDCA on oxidative stress in tunicamycin-induced DRG neurons. The oxidative stress response of DRG neurons following tunicamycin stimulation with or without TUDCA pre-incubation was determined by detecting ROS, LDH, MDA and GSH levels. As shown in Fig. 2, levels of ROS, LDH, MDA and GSH were not influenced by TUDCA alone at 250 μM. The levels of ROS, MDA and LDH in DRG neurons were increased by tunicamycin, whereas the levels of the antioxidant GSH were decreased. Tunicamycin-induced free radical generation and oxidative stress was markedly suppressed by pretreatment with TUDCA (250 μM) for 24 h, and the decrease in GSH concentration was also relieved (Fig. 2).

TUDCA protects DRG neurons from apoptosis. To explore whether apoptosis of DRG neurons followed exposure to tunicamycin, TUNEL staining was performed. As shown in Fig. 3, the percentages of TUNEL-positive apoptotic cells were increased up to 60% in groups exposed to tunicamycin compared with the TUN only group; however, there was no change when cells were exposed to TUDCA alone. As expected, pretreatment with TUDCA reduced the occurrence of apoptosis in tunicamycin-treated DRG neurons (Fig. 3), indicating the neuroprotective role of TUDCA.

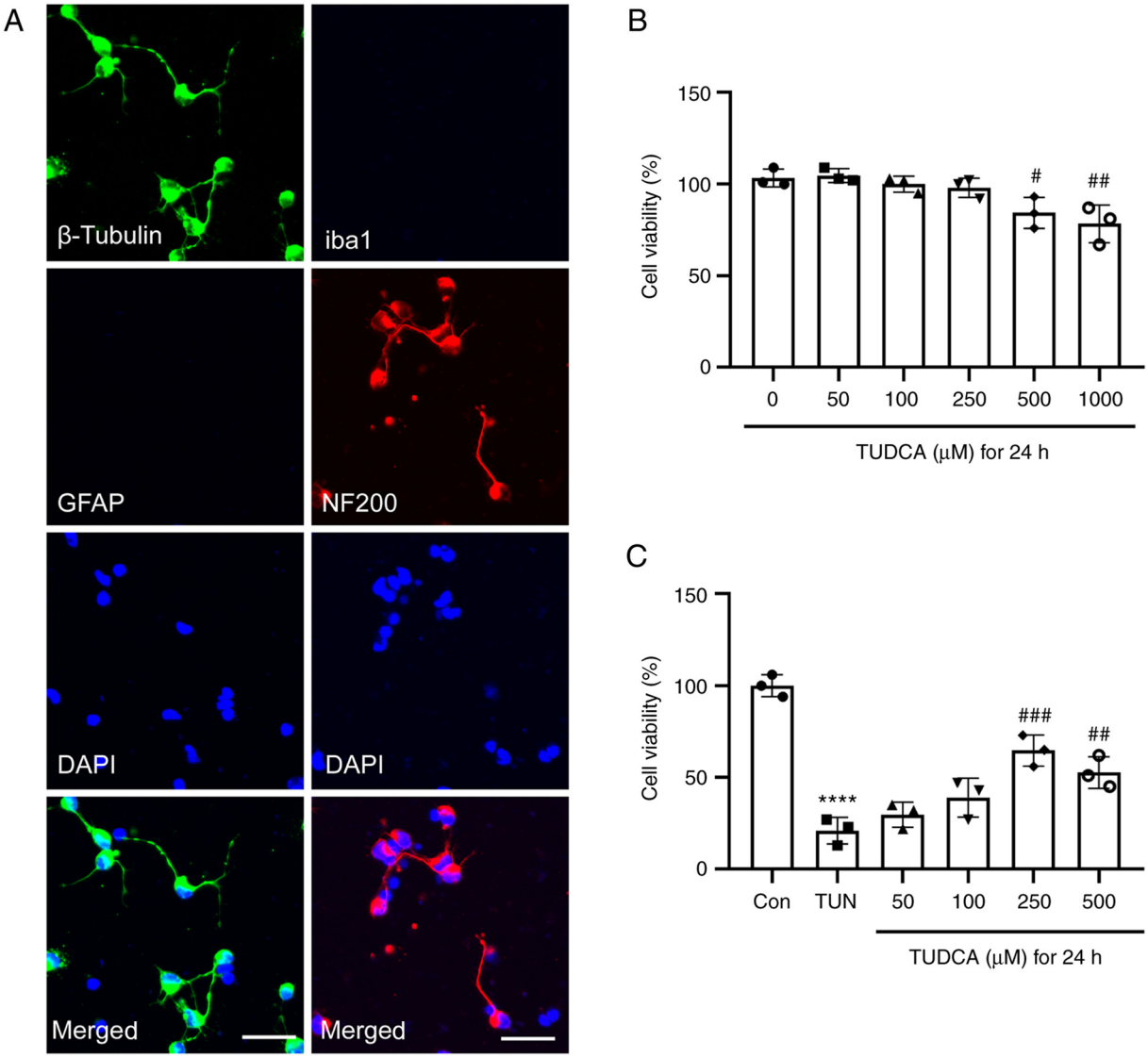

Figure 1. Effect of TUDCA on the viability of DRG neurons. (A) Immunofluorescence staining of rat DRG neurons *in vitro*. DRG neurons were stained with β-tubulin (green), GFAP (red), Iba1 (green) and NF200 (red), and nuclei were detected with DAPI staining (blue). Representative images from three experiments are shown. Scale bar, 20 μm. (B) Effect of different concentrations of TUDCA on the viability of DRG neurons. (C) Tunicamycin-induced cytotoxicity in DRG neurons was suppressed by TUDCA. Data were obtained from three independent experiments and are expressed as the mean ± SEM. The control group was set at 100%. ****P<0.0001 vs. control group; $^{\#}$P<0.05, $^{\#\#}$P<0.01, $^{\#\#\#}$P<0.001 vs. TUN group. DRG, dorsal root ganglion; TUDCA, tauroursodeoxycholic acid; GFAP, glial fibrillary acidic protein; Iba1, ionized calcium binding adaptor molecule 1; NF200, neurofilament 200; TUN, tunicamycin.

Caspase activities and the expression levels of apoptosis-related genes were examined by caspase-Glo assay and RT-qPCR, respectively. A marked increase in the activities of caspase-3 and caspase-9 was found in tunicamycin-treated DRG neurons, whereas pretreatment with TUDCA induced a modest but significant reduction in caspase-3 and caspase-9 activities as compared with the tunicamycin group (Fig. 4A and B), which was consistent with the TUNEL staining results. Similar trends were also found regarding the expression levels of the pro-apoptotic factors Bax, DP5 and PUMA. TUDCA suppressed the expression levels of Bax, DP5, cleaved caspase-3 and PUMA in neurons induced by tunicamycin without affecting the expression of total caspase-3 (Fig. 4C and E-L). By contrast, the expression levels of Bcl-2, an apoptotic suppressor, were decreased by tunicamycin, which was reversed by the addition of TUDCA (Fig. 4D). DRG neuronal apoptosis was also induced by thapsigargin and a similar protective effect of TUDCA was observed (Fig. S1).

TUDCA suppresses tunicamycin-induced ER stress activation in DRG neurons. Tunicamycin has been shown to cause ER stress in a variety of cells (22-24). In order to investigate whether ER stress response was involved in the anti-apoptotic effect of TUDCA in DRG neurons, the protein expression levels of C/EBP homologous protein (CHOP), glucose-regulated protein 78 (GRP78) and cleaved caspase-12 were assessed by western blotting. The CHOP pathway has been suggested to be the main pathway through which apoptosis is induced during ER stress (25). The protein expression levels of CHOP and GRP78 were upregulated in tunicamycin-treated DRG neurons as compared with the control group; however, the upregulation of CHOP and GRP78 by tunicamycin was suppressed by TUDCA pretreatment (Fig. 5A-C). In addition, elevated levels of cleaved

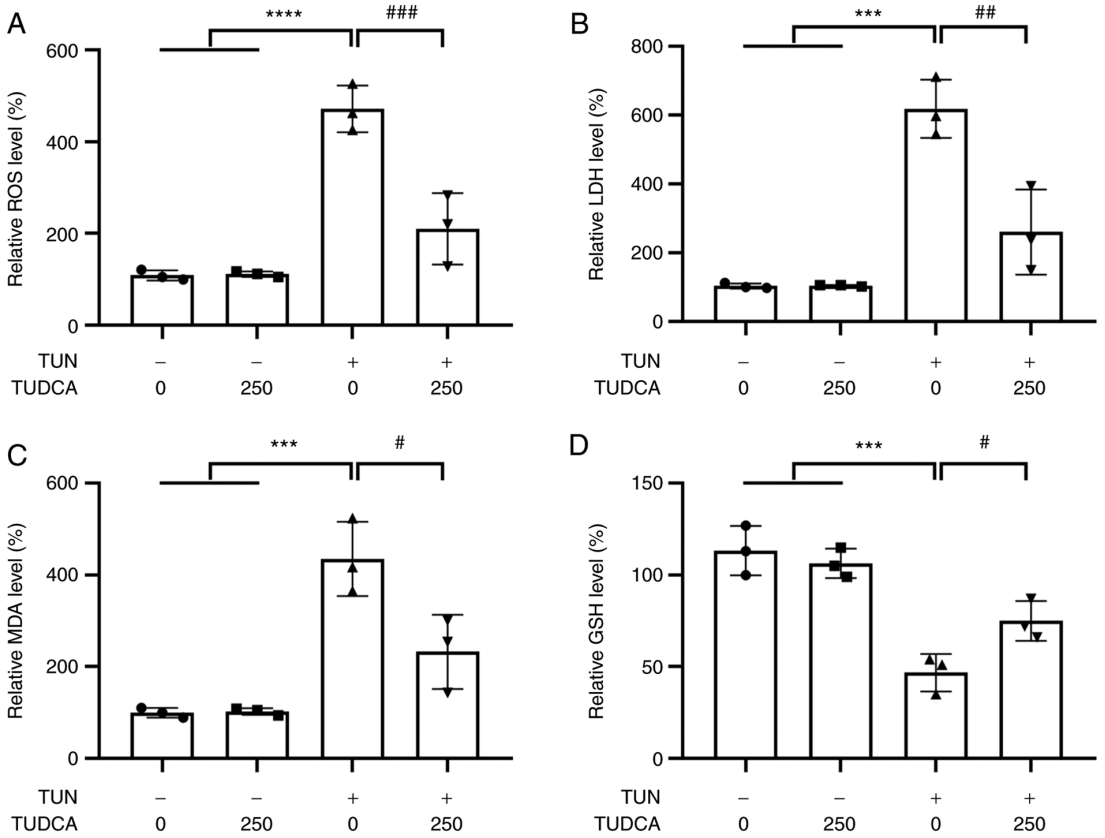

Figure 2. Effect of TUDCA on TUN-induced oxidative damage in DRG neurons. DRG neurons were treated with 250 μM TUDCA for 24 h prior to a 24 h-stimulation with TUN (0.75 μg/ml). Relative (A) ROS, (B) LDH, (C) MDA and (D) GSH levels in DRG neurons were detected 24 h after the indicated exposure. The control group was set at 100%. Data were obtained from three independent experiments and are expressed as the mean ± SEM. ***P<0.001, ****P<0.0001 vs. control group; $^{\#}$P<0.05, $^{\#\#}$P<0.01 and $^{\#\#\#}$P<0.001 vs. TUN group. DRG, dorsal root ganglion; TUDCA, tauroursodeoxycholic acid; TUN, tunicamycin; ROS, reactive oxygen species; MDA, malondialdehyde; LDH, lactate dehydrogenase; GSH, glutathione.

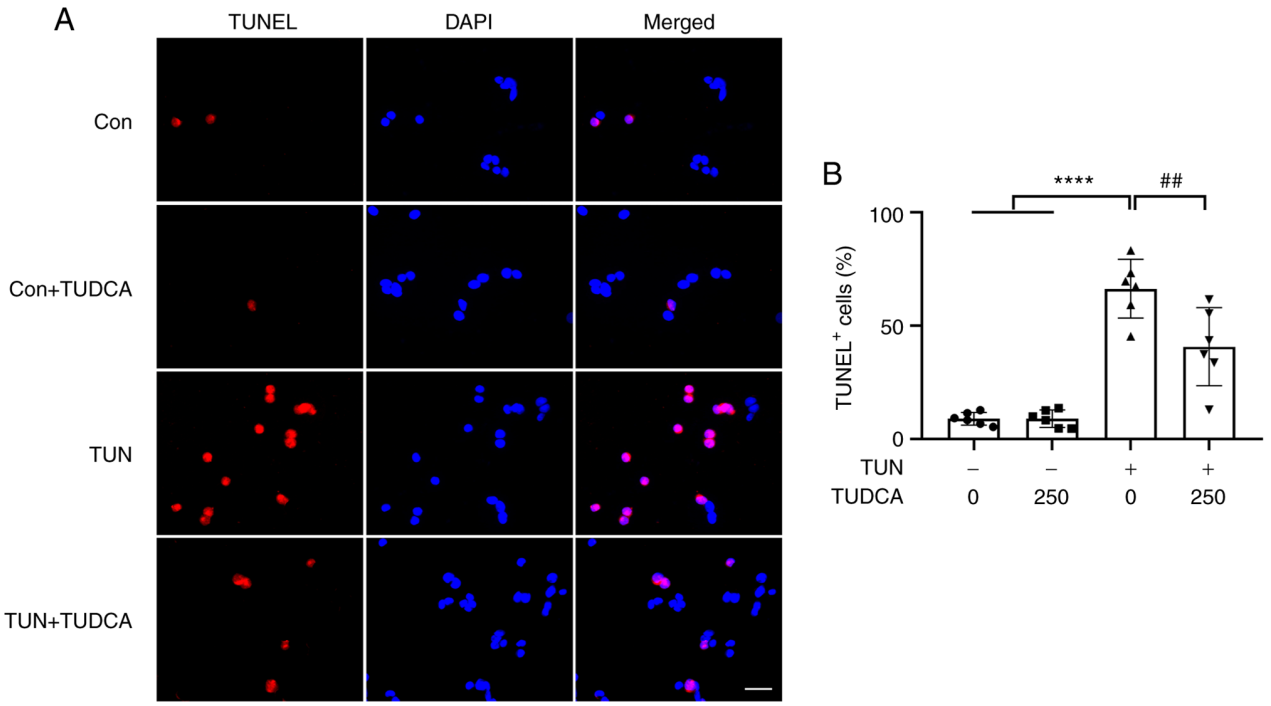

Figure 3. Effect of TUDCA on the apoptosis of TUN-induced DRG neurons. Apoptotic DRG neurons were measured by TUNEL staining after TUN and/or TUDCA stimulus. (A) Representative images of TUNEL staining (red) in control, TUDCA, TUN and TUN + TUDCA groups. Nuclear phenotype was also investigated via DAPI staining (blue). Scale bar, 20 μm. (B) Quantitative analysis of percentages of apoptotic cells after TUDCA and/or TUN treatment. Data were obtained from three independent experiments and are expressed as the mean ± SEM. ****P<0.0001 vs. control group; $^{\#\#}$P<0.01 vs. TUN group. DRG, dorsal root ganglion; TUDCA, tauroursodeoxycholic acid; TUN, tunicamycin.

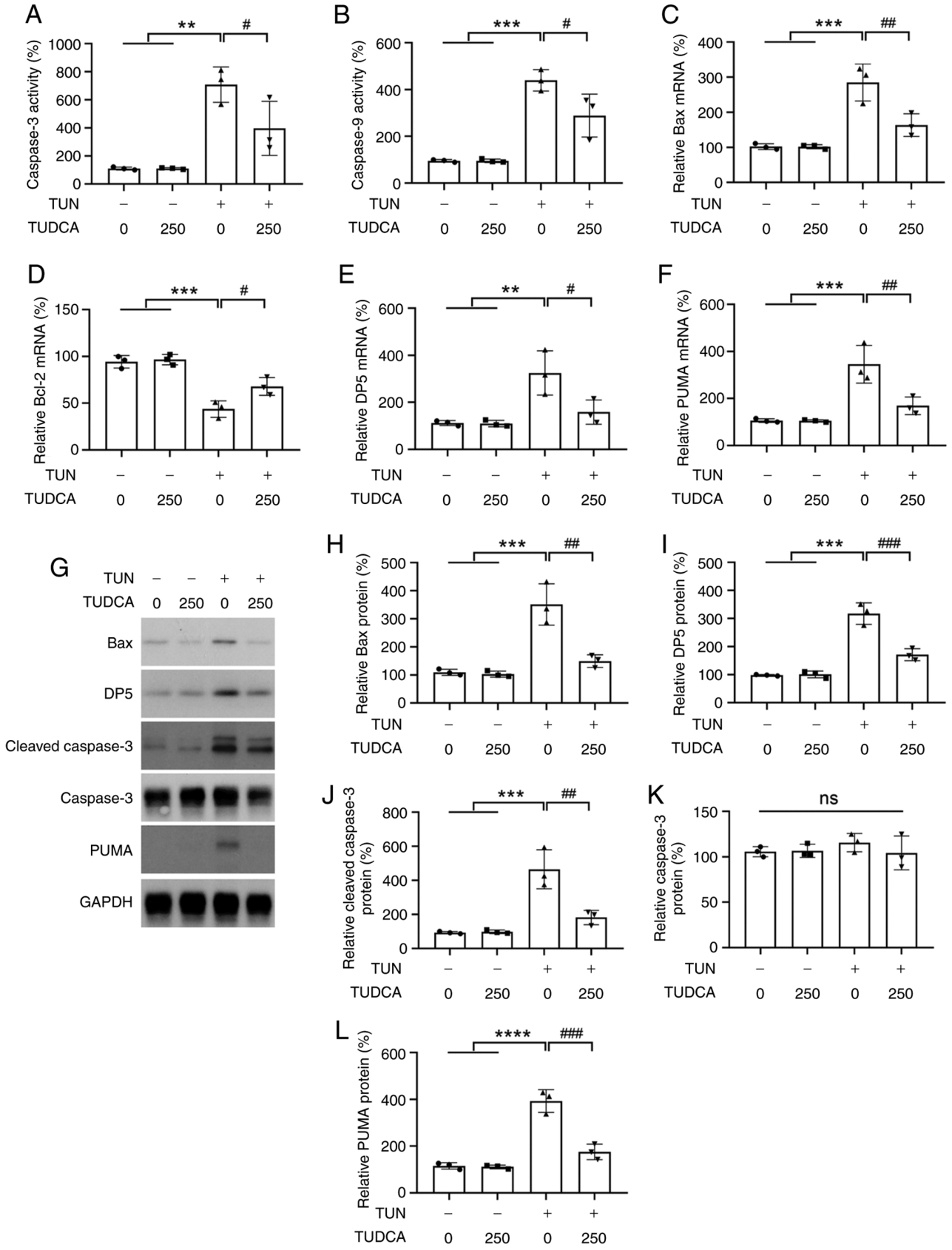

Figure 4. Changes in the levels of apoptosis-related factors in DRG neurons after TUDCA and TUN treatment. (A) Caspase-3 and (B) caspase-9 activity in DRG neurons after TUDCA and TUN treatment was examined by Caspase-Glo kits. Relative mRNA expression levels of (C) Bax, (D) Bcl-2, (E) DP5 and (F) PUMA were analyzed by reverse transcription-quantitative PCR. β-actin was used as an endogenous control. (G) Protein expression levels of Bax, DP5, caspase-3 and PUMA were determined by western blot analysis. Bar charts demonstrate the relative protein expression levels of (H) Bax, (I) DP5, (J) cleaved caspase-3, (K) total caspase-3 and (L) PUMA normalized to GAPDH or total caspase-3 for each group by densitometry. The control group was set at 100%. Data were obtained from three independent experiments and are expressed as the mean ± SEM. The control group was set at 100%. **P<0.01, ***P<0.001, ****P<0.00001 vs. control group; $^{\#}$P<0.05, $^{\#\#}$P<0.01 and $^{\#\#\#}$P<0.001 vs. TUN group. DRG, dorsal root ganglion; TUDCA, tauroursodeoxycholic acid; TUN, tunicamycin.

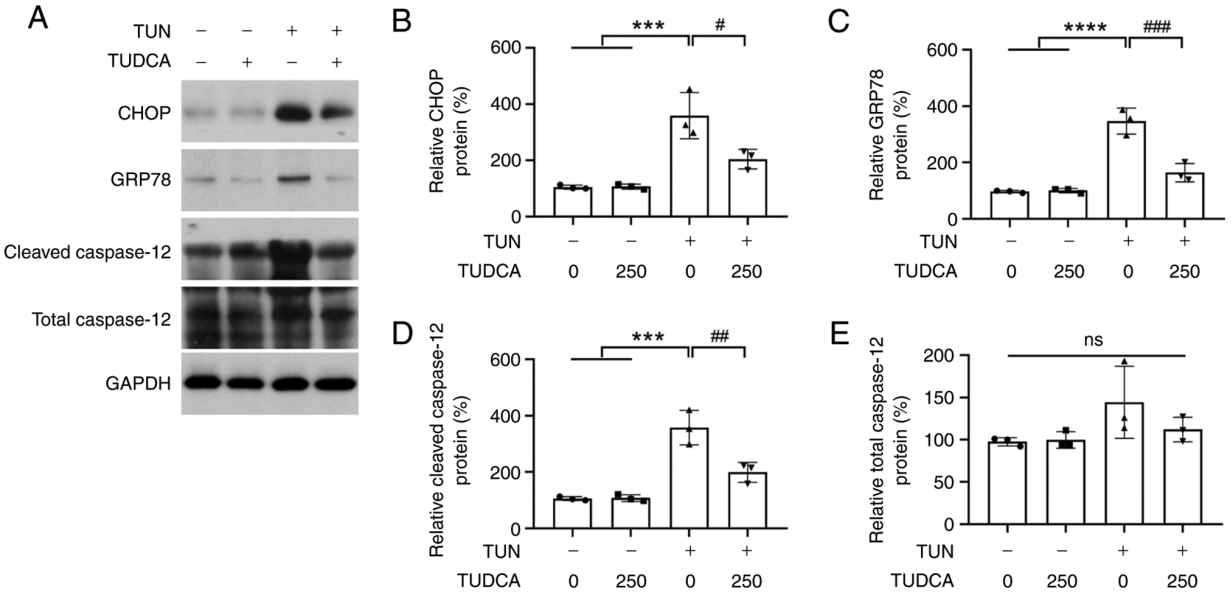

Figure 5. TUN-induced ER stress activation is suppressed by TUDCA. (A) Western blotting was performed to detect the protein expression levels of CHOP, GRP78, cleaved caspase-12 and total caspase-12. The bar charts demonstrate the ratio of (B) CHOP, (C) GRP78, (D) total caspase-12 and (E) cleaved caspase-12 protein relative to GAPDH for each group by densitometry. The control group was set at 100%. Data were obtained from three independent experiments and are expressed as the mean ± SEM. ***P<0.001, ****P<0.0001 vs. control group; $^{\#}$P<0.05, $^{\#\#}$P<0.01 and $^{\#\#\#}$P<0.001 vs. TUN group. TUDCA, tauroursodeoxycholic acid; TUN, tunicamycin; CHOP, C/EBP homologous protein; GRP78, glucose-regulated protein 78.

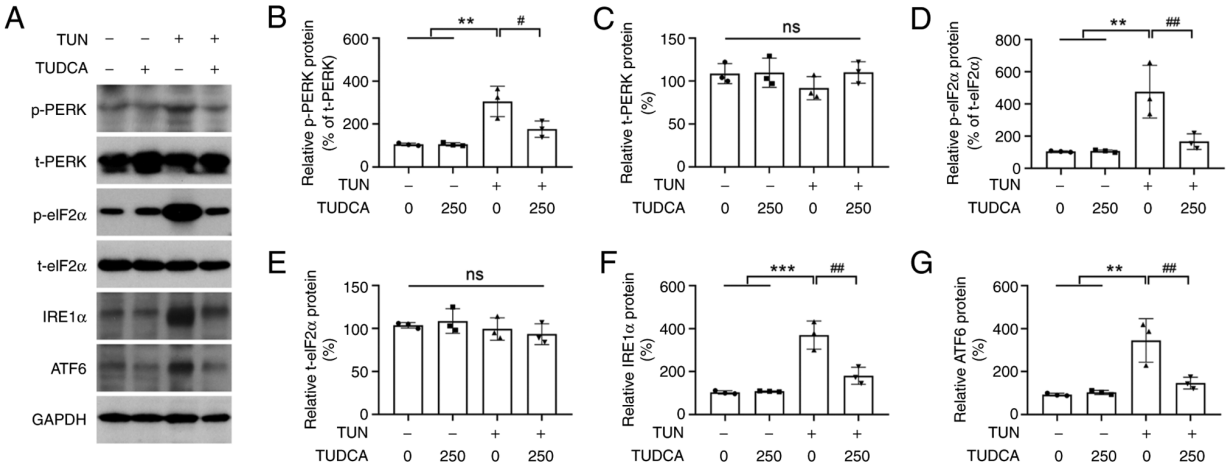

Figure 6. Effect of TUDCA on the UPR signaling pathway in DRG neurons. (A) Protein expression levels of p-PERK, t-PERK, p-eIF2α, t-eIF2α, IRE1α and ATF6 in DRG neurons following TUN and TUDCA treatment were evaluated by western blotting. Bar charts show the ratio of (B) p-PERK, (C) t-PERK, (D) p-eIF2α, (E) t-eIF2α, (F) IRE1α and (G) ATF6, as determined by densitometry. GAPDH was used as an internal reference; p-PERK levels were normalized to t-PERK levels and p-eIF2α levels were normalized to t-PERK levels. The control group was set at 100%. Data were obtained from three independent experiments and are expressed as the mean ± SEM. **P<0.01, ***P<0.001 vs. control group; $^{\#}$P<0.05 and $^{\#\#}$P<0.01 vs. TUN group. DRG, dorsal root ganglion; TUDCA, tauroursodeoxycholic acid; TUN, tunicamycin; PERK, protein kinase R-like ER kinase; p, phosphorylated; t, total.

caspase-12, a key mediator of ER stress-induced apoptosis, were also observed in DRG neurons following tunicamycin stimulation and reversed by TUDCA pretreatment (Fig. 5A and D). There was no difference in total caspase-12 levels in tunicamycin- or TUDCA-treated DRG neurons as compared with that in the vehicle group (Fig. 5A and E).

Effect of TUDCA on the UPR pathway in tunicamycin-induced DRG neurons. Under ER stress, the UPR is activated to maintain ER and cellular function, and accumulation of unfolded proteins is sensed through ER transmembrane protein sensors PERK, IRE1α and ATF6. To better understand how the UPR pathways contribute to the neuroprotective effect of TUDCA on DRG neurons, the activation of PERK, IRE1α and ATF6 was investigated by western blotting. No obvious expression changes in the phosphorylation of PERK (p-PERK) and eIF2α (p-eIF2α; a signal downstream of PERK), as well as in ATF6 levels, were observed among the control and 250 μM TUDCA groups. By contrast, tunicamycin treatment increased the expression levels of p-PERK and p-eIF2α, as well as IRE1α and ATF6 (Fig. 6). Moreover, activation of the UPR pathways was inhibited by pre-incubation of DRG neurons with TUDCA before tunicamycin exposure (Fig. 6).

Discussion

TUDCA has been shown to be the major active ingredient of black bear bile, which has been utilized to treat liver- and eye-related illnesses for centuries in traditional Chinese medicine (2). TUDCA is more hydrophilic and a more abundant naturally produced bile acid in humans and bears than UDCA. A large number of potential uses for TUDCA has been reported in studies of animal models (2,26,27). Notably, TUDCA has attracted much attention from researchers as a neuroprotective agent. The protective role of TUDCA in retinal degeneration has been extensively reported in preclinical studies, and intraperitoneal injection of TUDCA has been reported to protect against oxidative stress-induced retinal degeneration (28), to promote neuronal survival after experimental retinal detachment, to be closely associated with oxidative stress and caspase activities (29), to reduce Brn311-labeled retinal ganglion cell loss and to notably enhance GAP-43-positive axons in a rat optic nerve crush model (30). In addition, several studies have demonstrated neuroprotective roles of TUDCA in the brain. Chronic feeding of TUDCA has been shown to interfere with amyloid-β peptide production in APP/PS1 mice (14), indicating its potential role in the treatment of Alzheimer's disease. Wu *et al* (31) reported that TUDCA administration attenuated neuronal apoptosis and improved neurological functions in the pathogenesis of a subarachnoid hemorrhage model. However, little is currently known about the effect of TUDCA on rat DRG neurons. To the best of our knowledge, the present study is the first to examine the neuroprotective effect of TUDCA on tunicamycin-induced ER stress and apoptosis of primary DRG neurons.

The present study showed that preincubation with TUDCA (250 μM) markedly attenuated tunicamycin-induced cell death of primary DRG neurons, as demonstrated by CellTiter-Blue assay, TUNEL staining and LDH assay. When the concentration was ≤250 μM, TUDCA exhibited no cytotoxicity in DRG neurons. These findings indicated that TUDCA had a cytoprotective effect on DRG neurons against tunicamycin-induced toxicity. These data were consistent with the results of previous studies conducted in other types of neurons, such as retinal (32), primary cortical (33) and dopamine neurons (34).

Despite these observations, little is currently known about the exact molecular mechanism underlying these phenomena. In general, inhibition of ER stress and stabilization of the UPR pathways have been considered important mechanisms underlying the biological functions of TUDCA (35-37). Notably, TUDCA has been used as an inhibitor of ER stress in previous studies (38,39). The present study revealed that tunicamycin-induced ER stress activation and TUNEL-positive cells were suppressed by pretreatment with TUDCA. In the presence of tunicamycin, apoptosis of neurons was induced by ROS-mediated ER stress, indicated by the enhancing of activities of caspase-3 and caspase-9, and increasing of CHOP, GRP78 and ER resident cleaved caspase-12 in DRG neurons exposed to tunicamycin. Both the activation of ER stress and the enhanced caspase activities were reversed by TUDCA. According to these data, it is strongly conceivable that TUDCA rescued ER stress-associated apoptosis in tunicamycin-treated DRG neurons.

Considerable evidence has shown that ER stress is initiated by the accumulation of unfolded or misfolded proteins in the ER lumen. Consequently, PERK, IRE1α and ATF6 sense the fidelity of protein folding in the ER lumen and activate the UPR to eliminate or repair these misfolded proteins. In severe cases, uncontrolled UPR can lead to cell death by activating the pro-apoptotic signaling pathways. In healthy cells, the ER environment is much more oxidative than the cytosolic compartment, which favors protein folding (40,41). Crosstalk between ER stress and oxidative stress has been extensively reported in physiological and pathological conditions (42,43). The present study evaluated the oxidative stress in DRG neurons by detecting the levels of ROS, MDA and the antioxidant GSH. As expected, the levels of ROS and MDA in DRG neurons stimulated with tunicamycin were markedly higher, whereas the levels of GSH were reduced compared with those in the control group. However, these phenotypes could be alleviated by pretreatment with TUDCA, suggesting that TUDCA protected primary DRG neurons from oxidative stress *in vitro*. Using western blot analysis, the activation of three branches of the UPR (PERK, eIF2α, and ATF6) was assessed; all of these pathways were activated in DRG neurons following tunicamycin exposure and were reversed by TUDCA pretreatment (Fig. 7), as determined by changes in p-PERK, p-eIF2α, IRE1α and ATF6 expression. These findings indicated that ER stress and the UPR may be implicated in the mechanism that leads to cell apoptosis of tunicamycin-induced DRG neurons and the neuroprotective role of TUDCA.

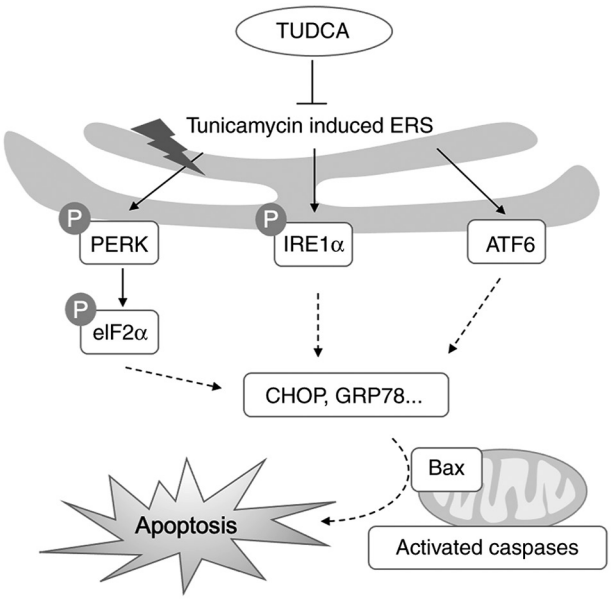

Figure 7. Schematic diagram of the role of TUDCA in dorsal root ganglion neurons. TUDCA inhibited ERS-induced activation of PERK, IRE1α, ATF6 and ERS-associated apoptosis. TUDCA, tauroursodeoxycholic acid; PERK, protein kinase R-like ER kinase; CHOP, C/EBP homologous protein; GRP78, glucose-regulated protein 78; ERS, ER stress.

The present study revealed that the expression of the canonical transducer of the UPR, ATF6, was increased in DRG neurons following tunicamycin exposure and was reversed by TUDCA. These findings are consistent with the findings of Nakada *et al* (44), which reported that TUDCA may directly bind to ATF6 and reduce its protein levels. In the present study, TUDCA also decreased the phosphorylation levels of eIF2α and PERK, which may not only exert biological effects through ATF6, but may also act through other upstream targets.

TUDCA has been reported to alleviate rifampicin-induced injury in liver cancer cells by increasing the expression of bile acid transporters and enhancing the Nrf2-mediated adaptive response (45). The exact target of TUDCA in DRG neurons still needs to be further investigated.

Taken together, the present study provided evidence that TUDCA prevented ER stress-associated apoptosis in tunicamycin-induced DRG neurons. TUDCA has been used to treat primary biliary cholangitis, and has good safety and effectiveness in clinical practice. However, the study of its effects on the nervous system is still in its early stage. The protective effect and therapeutic value of TUDCA in DRG neurons still need to be further evaluated in spinal cord or sciatic nerve injury animal models. Although the present study and a range of other studies have shown the positive effects of TUDCA in cell cultures and pre-clinical studies, there are certain limitations restraining its clinical use, such as the relatively high TUDCA absorption capacity of hepatocytes; therefore, researchers should consider the effects of TUDCA on liver function when using TUDCA to treat neurological diseases.

Acknowledgements

Not applicable.

Funding

This study was supported by the Youth Project of Shanghai Municipal Health and Family Planning Commission (grant no. 2018Y0141).

Availability of data and materials

The datasets used and/or analyzed during the current study are available from the corresponding author on reasonable request.

Authors' contributions

GC and XH designed the study and reviewed the manuscript. FC and ZG acquired the majority of the data and drafted the manuscript. NL and ZY analyzed the data and revised the manuscript. RW and YZ interpreted the data, provided literature support and revised the manuscript. All authors have read and approved the final manuscript. RW and YZ confirm the authenticity of all the raw data.

Ethics approval and consent to participate

Rats were used according to the Guide for the Care and Use of Laboratory Animals, 8th edition (46) and the present study was approved by the Institutional Animal Care and Use Committee of Fudan University (approval no. 20200524087).

Patient consent for publication

Not applicable.

Competing interests

The authors declare that they have no competing interests.

References

1. Ma H, Zeng M, Han Y, Yan H, Tang H, Sheng J, Hu H, Cheng L, Xie Q, Zhu Y, *et al*: A multicenter, randomized, double-blind trial comparing the efficacy and safety of TUDCA and UDCA in Chinese patients with primary biliary cholangitis. Medicine (Baltimore) 95: e5391, 2016.
2. Kusaczuk M: Tauroursodeoxycholate-bile acid with chaperoning activity: Molecular and cellular effects and therapeutic perspectives. Cells 8: 1471, 2019.
3. Ozcan U, Yilmaz E, Ozcan L, Furuhashi M, Vaillancourt E, Smith RO, Görgün CZ and Hotamisligil GS: Chemical chaperones reduce ER stress and restore glucose homeostasis in a mouse model of type 2 diabetes. Science 313: 1137-1140, 2006.
4. Fonseca I, Gordino G, Moreira S, Nunes MJ, Azevedo C, Gama MJ, Rodrigues E, Rodrigues CMP and Castro-Caldas M: Tauroursodeoxycholic acid protects against mitochondrial dysfunction and cell death via mitophagy in human neuroblastoma cells. Mol Neurobiol 54: 6107-6119, 2017.
5. Li P, Fu D, Sheng Q, Yu S, Bao X and Lv Z: TUDCA attenuates intestinal injury and inhibits endoplasmic reticulum stress-mediated intestinal cell apoptosis in necrotizing enterocolitis. Int Immunopharmacol 74: 105665, 2019.
6. Yamaguchi Y, Oh-Hashi K, Matsuoka Y, Takemura H, Yamakita S, Matsuda M, Sawa T and Amaya F: Endoplasmic reticulum stress in the dorsal root ganglion contributes to the development of pain hypersensitivity after nerve injury. Neuroscience 394: 288-299, 2018.
7. Tan HP, Guo Q, Hua G, Chen JX and Liang JC: Inhibition of endoplasmic reticulum stress alleviates secondary injury after traumatic brain injury. Neural Regen Res 13: 827-836, 2018.
8. Yin Y, Sun G, Li E, Kiselyov K and Sun D: ER stress and impaired autophagy flux in neuronal degeneration and brain injury. Ageing Res Rev 34: 3-14, 2017.
9. Li W, Li W, Leng Y, Xiong Y and Xia Z: Ferroptosis is involved in diabetes myocardial ischemia/reperfusion injury through endoplasmic reticulum stress. DNA Cell Biol 39: 210-225, 2020.
10. Yang Y, Zhou Q, Gao A, Chen L and Li L: Endoplasmic reticulum stress and focused drug discovery in cardiovascular disease. Clin Chim Acta 504: 125-137, 2020.
11. Ashraf NU and Sheikh TA: Endoplasmic reticulum stress and oxidative stress in the pathogenesis of non-alcoholic fatty liver disease. Free Radic Res 49: 1405-1418, 2015.
12. Lebeaupin C, Vallée D, Hazari Y, Hetz C, Chevet E and Bailly-Maitre B: Endoplasmic reticulum stress signalling and the pathogenesis of non-alcoholic fatty liver disease. J Hepatol 69: 927-947, 2018.
13. Chen X and Cubillos-Ruiz JR: Endoplasmic reticulum stress signals in the tumour and its microenvironment. Nat Rev Cancer 21: 71-88, 2021.
14. Nunes AF, Amaral JD, Lo AC, Fonseca MB, Viana RJ, Callaerts-Vegh Z, D'Hooge R and Rodrigues CM: TUDCA, a bile acid, attenuates amyloid precursor protein processing and amyloid-β deposition in APP/PS1 mice. Mol Neurobiol 45: 440-454, 2012.
15. Radford H, Moreno JA, Verity N, Halliday M and Mallucci GR: PERK inhibition prevents tau-mediated neurodegeneration in a mouse model of frontotemporal dementia. Acta Neuropathol 130: 633-642, 2015.
16. Valenzuela V, Jackson KL, Sardi SP and Hetz C: Gene therapy strategies to restore ER proteostasis in disease. Mol Ther 26: 1404-1413, 2018.
17. Lin CR, Yang CH, Huang CE, Wu CH, Chen YS, Sheen-Chen SM, Huang HW and Chen KH: GADD45A protects against cell death in dorsal root ganglion neurons following peripheral nerve injury. J Neurosci Res 89: 689-699, 2011.
18. Wiberg R, Novikova LN and Kingham PJ: Evaluation of apoptotic pathways in dorsal root ganglion neurons following peripheral nerve injury. Neuroreport 29: 779-785, 2018.
19. Chen F, Wu R, Zhu Z, Yin W, Xiong M, Sun J, Ni M, Cai G and Zhang X: Wogonin protects rat dorsal root ganglion neurons against tunicamycin-induced ER stress through the PERK-eIF2α-ATF4 signaling pathway. J Mol Neurosci 55: 995-1005, 2015.
20. Levin E, Diekmann H and Fischer D: Highly efficient transduction of primary adult CNS and PNS neurons. Sci Rep 6: 38928, 2016.
21. Livak KJ and Schmittgen TD: Analysis of relative gene expression data using real-time quantitative PCR and the 2(-Delta Delta C(T)) method. Methods 25: 402-408, 2001.

22. Yakin M, Seo B and Rich A: Tunicamycin-induced endoplasmic reticulum stress up-regulates tumour-promoting cytokines in oral squamous cell carcinoma. Cytokine 120: 130-143, 2019.
23. Wu F, Zhang R, Feng Q, Cheng H, Xue J and Chen J: (-)-Clausenamide alleviated ER stress and apoptosis induced by OGD/R in primary neuron cultures. Neurol Res 42: 730-738, 2020.
24. Quan X, Wang J, Liang C, Zheng H and Zhang L: Melatonin inhibits tunicamycin-induced endoplasmic reticulum stress and insulin resistance in skeletal muscle cells. Biochem Biophys Res Commun 463: 1102-1107, 2015.
25. Hu H, Tian M, Ding C and Yu S: The C/EBP homologous protein (CHOP) transcription factor functions in endoplasmic reticulum stress-induced apoptosis and microbial infection. Front Immunol 9: 3083, 2018.
26. Zangerolamo L, Vettorazzi JF, Solon C, Bronczek GA, Engel DF, Kurauti MA, Soares GM, Rodrigues KS, Velloso LA, Boschero AC, *et al*: The bile acid TUDCA improves glucose metabolism in streptozotocin-induced Alzheimer's disease mice model. Mol Cell Endocrinol 521: 111116, 2021.
27. Lu Q, Jiang Z, Wang Q, Hu H and Zhao G: The effect of tauroursodeoxycholic acid (TUDCA) and gut microbiota on murine gallbladder stone formation. Ann Hepatol 23: 100289, 2021.
28. Oveson BC, Iwase T, Hackett SF, Lee SY, Usui S, Sedlak TW, Snyder SH, Campochiaro PA and Sung JU: Constituents of bile, bilirubin and TUDCA, protect against oxidative stress-induced retinal degeneration. J Neurochem 116: 144-153, 2011.
29. Mantopoulos D, Murakami Y, Comander J, Thanos A, Roh M, Miller JW and Vavvas DG: Tauroursodeoxycholic acid (TUDCA) protects photoreceptors from cell death after experimental retinal detachment. PLoS One 6: e24245, 2011.
30. Kitamura Y, Bikbova G, Baba T, Yamamoto S and Oshitari T: In vivo effects of single or combined topical neuroprotective and regenerative agents on degeneration of retinal ganglion cells in rat optic nerve crush model. Sci Rep 9: 101, 2019.
31. Wu H, Yu N, Wang X, Yang Y and Liang H: Tauroursodeoxycholic acid attenuates neuronal apoptosis via the TGR5/SIRT3 pathway after subarachnoid hemorrhage in rats. Biol Res 53: 56, 2020.
32. Bikbova G, Oshitari T, Baba T and Yamamoto S: Combination of neuroprotective and regenerative agents for AGE-induced retinal degeneration: In vitro study. Biomed Res Int 2017: 8604723, 2017.
33. Hou Y, Luan J, Huang T, Deng T, Li X, Xiao Z, Zhan J, Luo D, Hou Y, Xu L and Lin D: Tauroursodeoxycholic acid alleviates secondary injury in spinal cord injury mice by reducing oxidative stress, apoptosis, and inflammatory response. J Neuroinflammation 18: 216, 2021.
34. Duan WM, Rodrigures CMP, Zhao LR, Steer CJ and Low WC: Tauroursodeoxycholic acid improves the survival and function of nigral transplants in a rat model of Parkinson's disease. Cell Transplant 11: 195-205, 2002.
35. Lee JH, Yoon YM and Lee SH: TUDCA-treated mesenchymal stem cells protect against ER stress in the hippocampus of a murine chronic kidney disease Model. Int J Mol Sci 20: 613, 2019.
36. Zhao H, Wang Y, Li B, Zheng T, Liu X, Hu BH, Che J, Zhao T, Chen J, Hatzoglou M, *et al*: Role of endoplasmic reticulum stress in otitis media. Front Genet 11: 495, 2020.
37. Wen Y, Zong S, Liu T, Du P, Li H and Xiao H: Tauroursodeoxycholic acid attenuates cisplatin-induced ototoxicity by inhibiting the accumulation and aggregation of unfolded or misfolded proteins in the endoplasmic reticulum. Toxicology 453: 152736, 2021.
38. Kim EH and Park PH: Globular adiponectin protects rat hepatocytes against acetaminophen-induced cell death via modulation of the inflammasome activation and ER stress: Critical role of autophagy induction. Biochem Pharmacol 154: 278-292, 2018.
39. Yu X, Wang T, Zhu M, Zhang L, Zhang F, Jing E, Ren Y, Wang Z, Xin Z and Lin T: Transcriptome and physiological analyses for revealing genes involved in wheat response to endoplasmic reticulum stress. BMC Plant Biol 19: 193, 2019.
40. Magallón M, Carrión AE, Bañuls L, Pellicer D, Castillo S, Bondía S, Navarro-García MM, González C and Dasí F: Oxidative stress and endoplasmic reticulum stress in rare respiratory diseases. J Clin Med 10: 1268, 2021.
41. Hwang C, Sinskey AJ and Lodish HF: Oxidized redox state of glutathione in the endoplasmic reticulum. Science 257: 1496-1502, 1992.
42. Victor P, Umapathy D, George L, Juttada U, Ganesh GV, Amin KN, Viswanathan V and Ramkumar KM: Crosstalk between endoplasmic reticulum stress and oxidative stress in the progression of diabetic nephropathy. Cell Stress Chaperones 26: 311-321, 2021.
43. Cansler SM and Evanson NK: Connecting endoplasmic reticulum and oxidative stress to retinal degeneration, TBI, and traumatic optic neuropathy. J Neurosci Res 98: 571-574, 2020.
44. Nakada EM, Bhakta NR, Korwin-Mihavics BR, Kumar A, Chamberlain N, Bruno SR, Chapman DG, Hoffman SM, Daphtary N, Aliyeva M, *et al*: Conjugated bile acids attenuate allergen-induced airway inflammation and hyperresponsiveness by inhibiting UPR transducers. JCI Insight 4: e98101, 2019.
45. Zhang W, Chen L, Feng H, Wang W, Cai Y, Qi F, Tao X, Liu J, Shen Y, Ren X, *et al*: Rifampicin-induced injury in HepG2 cells is alleviated by TUDCA via increasing bile acid transporters expression and enhancing the Nrf2-mediated adaptive response. Free Radic Biol Med 112: 24-35, 2017.
46. National Research Council (US): Committee for the Update of the Guide for the Care and Use of Laboratory Animals. Guide for the care and use of laboratory animals. 8th edition. National Academies Press, Washington, DC, 2011.